Int. J. Solids Structures, 1970, Vol. 6, pp. 1403 to 1412. Pergamon Press. Printed in Great Britain

STRESS PULSES PRODUCED DURING THE FRACTURE OF BRITTLE TENSILE SPECIMENS

J. W. PHILLIPS†

Research Associate, Division of Engineering, Brown University, Providence, Rhode Island

Abstract—A theoretical model similar to that used by Miklowitz is assumed for the fracture of uniaxial tensile specimens. For this model both symmetric and antisymmetric pulses are propagated away from the fracture zone. The theoretical predictions for surface strain are found to agree remarkably well with experimental results.

INTRODUCTION

MANY aspects of the relations between stress waves and the brittle fracture of solids have been investigated recently. Certain studies, like the determination of stress distributions around the tip of a running crack (e.g. [8, 11–13]), have involved a true interaction between the two phenomena, whereas other studies have tended to suppress this interaction either by treating fracture as the product of stress waves (e.g. [3, 9, 10]) or vice-versa. In the present paper, as in [14], fracture is treated as the cause of stress pulses. The specimen geometry and the type of loading are quite different from those used in [14], however; here the stress pulses produced in a loaded structural element when brittle fracture occurs at some cross-section are investigated. Specifically, a circular rod is treated because elastic wave propagation in such a specimen is fairly well understood [3–7].

The longitudinal pulses produced in metal wires when they fracture in uniaxial tension have been studied experimentally by Oi [1] in connection with strain gage response. However, in addition to the symmetric pulses which Oi observed, flexural (antisymmetric) pulses are produced even though there may be no initial bending of the rod. Miklowitz [15] recognized the existence of these flexural pulses and showed how they could reinforce reflected longitudinal pulses to produce secondary fractures. The present paper lends further experimental verification to Miklowitz' results, and presents an alternative (numerical) solution to the basic wave equations.

THEORY

Oi [1] restricted himself to a study of the *longitudinal* pulses produced during the brittle fracture of stretched wires, since his strain gages were used in pairs and were averaged. In the present study, glass rods with individually monitored strain gages were employed, and the presence of *flexural* pulses was also detected. The fractures appear to have started at suitable surface flaws, and thus the fracture patterns are not radially symmetric. In the following model, an attempt is made to relate observed flexural pulses (as well as longitudinal ones) to a fracture pattern centered at the rod surface [15].

† Now Assistant Professor, Department of Theoretical and Applied Mechanics, College of Engineering, University of Illinois, Urbana, Illinois.

An isotropic, linear elastic rod of radius R and of infinite length in the x-direction is initially in a state of uniaxial tension of magnitude σ_0. At time $t = 0$, fracture begins at a section of the rod which will be designated as $x = 0$. The fracture is assumed to initiate at a point on the rod surface and to propagate in the plane $x = 0$ with a circular crack front of constantly increasing radius. Behind the crack front the axial stress drops from its original value to zero, whereas everywhere in front of the crack the axial stress is assumed to remain at its initial value even though the crack propagation velocity v_c is less than the maximum wave speed in the material [8].

The normal stress resultant $F(x, t)$ acting at $x = 0$ is then a linear function of the ratio A/A_0 (see Fig. 1), and is given by [1]

$$F(0,t) = \begin{cases} \sigma_0 A_0, & \tau < 0 \\ \sigma_0 A_0 \left\{1 - \frac{1}{\pi}[4\tau^2 \cos^{-1}\tau + \cos^{-1}(1-\tau^2) \right. \\ \qquad \left. - 2\tau(1-\tau^2)^{1/2}]\right\}, & 0 \le \tau \le 1 \\ 0, & \tau > 1 \end{cases} \tag{1}$$

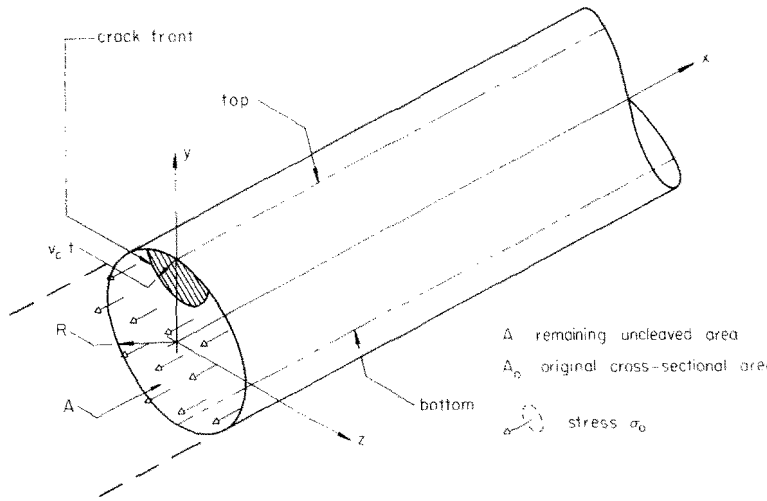

FIG. 1. Coordinate notation.

where τ is the dimensionless time $v_c t/2R$. A resultant bending moment is also induced at $x = 0$ since the resultant normal force does not act along the rod axis during fracture. It can be shown [2] that

$$M(0,t) = \begin{cases} 0, & \tau < 0 \\ 2\sigma_0 R^3 \left\{-\frac{1}{3}[1-(1-2\tau^2)^2]^{3/2} - \left[-2\tau^3\left(\frac{4}{3}(1+\tau)^2+1\right)(1-\tau^2)^{1/2} \right. \right. \\ \qquad \left. \left. + 2\tau^2\left(\frac{\pi}{2} - \sin^{-1}\tau\right)\right]\right\}, & 0 \le \tau \le 1 \\ 0, & \tau > 1 \end{cases} \tag{2}$$

The longitudinal and flexural stresses defined by

$$\sigma_L(x, t) = F(x, t)/A_0, \qquad \sigma_F(x, t) = M(x, t)R/I \tag{3a, b}$$

(where I is the moment of the original cross-section about a diameter, $\pi R^4/4$) are continuous functions of t at $x = 0$, as shown in Fig. 2. Due to symmetry, the shear force $S(x, t)$ vanishes at $x = 0$, i.e.

$$S(0, t) = 0, \qquad -\infty < t < \infty \tag{4}$$

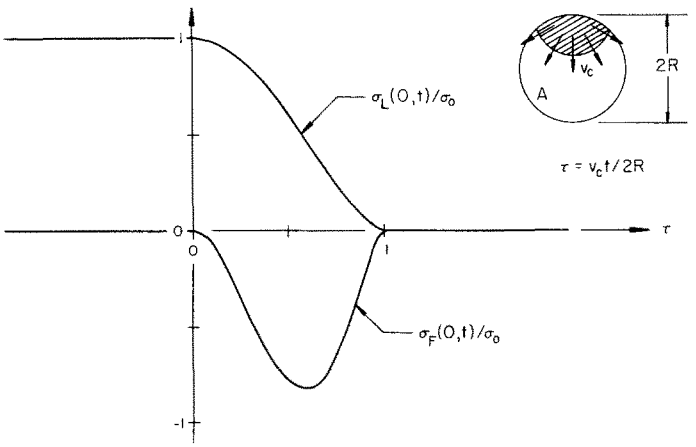

FIG. 2. Time variation of the equivalent stresses σ_L and σ_F acting at $x = 0$.

Equations (1, 2, 4) give the boundary conditions at $x = 0$ for the assumed fracture process. Experiments on crack propagation in glass [9] have shown that the maximum crack velocity is close to $0{\cdot}38c_0$ [8], where c_0 is the elastic bar velocity $(E/\rho)^{1/2}$ (E is Young's modulus and ρ the mass density of the material). Given that for glass, $c_0 = 2{\cdot}09 \times 10^5$ in./sec [3], one computes the duration of the pulse $2R/v_c$ to be not less than approximately 6 μsec for a 0·5 in. diameter rod. Smooth longitudinal stress pulses of this duration can be represented quite well by simple bar theory since for the fundamental longitudinal mode the dominant frequencies correspond to that part of the spectrum for which geometrical dispersion is negligible [3, 4]. Thus, simple bar theory is used. From this theory, the stress $\sigma_L(x, t)$ at any section $x \geq 0$ is given by

$$\sigma_L(x, t) = \sigma_L(0, t - x/c_0) \tag{5}$$

where $\sigma_L(0, t)$ is given by equation (3a) and the boundary condition (1).

The analysis of the flexural pulse which satisfies the boundary conditions (2) and (4) is based on the Timoshenko beam theory. According to this theory, if $w(x, t)$ denotes the transverse displacement of the rod from its initial position, then $w(x, t)$ obeys the linear partial differential equation (see [3], p. 53)

$$c_0^2K^2w_{,xxxx} - K^2(1+\varepsilon')w_{,xxtt} + \varepsilon'(K/c_0)^2w_{,tttt} + w_{,tt} = 0 \tag{6}$$

where K is the radius of gyration of the cross-section ($R/2$ in this case) and ε' is a constant dependent upon Poisson's ratio ν and the shape of the cross-section [5]. For a glass rod where $\nu = 0{\cdot}25$ ([3], p. 201), ε' takes the value 2·778.

Equation (6) is satisfied by $w(x, t)$ of the form

$$w(x, t) = \mathrm{Re}\{[W_1 \exp(-b_1 x) + W_2 \exp(-b_2 x)] \exp(i\omega t)\} \tag{7}$$

in which ω is circular frequency and W_1 amd W_2 are complex constants, provided that b_1 and b_2 satisfy

$$\left.\begin{matrix} b_1 \\ b_2 \end{matrix}\right\} = \frac{\omega}{\sqrt{2}c_0}\{-(1+\varepsilon') \mp [(1+\varepsilon')^2 + 4((c_0/\omega K)^2 - \varepsilon')]^{1/2}\}^{1/2} \tag{8}$$

Due to symmetry, only the two roots b_1 and b_2 corresponding to waves propagating or decaying in the direction of increasing x are considered. For all $\omega > 0$, root b_1 is pure imaginary and corresponds to the fundamental traveling mode. The dispersion relation $c = c(R/\Lambda)$, where c is the phase velocity $i\omega/b_1$ and Λ is the wavelength $2\pi c/\omega$, is shown as branch 1 in Fig. 3. This phase velocity curve is known to be in extremely good agreement with the one derived from the exact (three-dimensional elasticity) theory [3, 5] for a circular rod.

Root b_2 is respectively real, zero, or pure imaginary when ω is less than, equal to, or greater than a certain critical frequency ω_{cr} whose value from equation (8) is seen to be $c_0/(K\sqrt{\varepsilon'})$. Thus for $\omega > \omega_{cr}$, root b_2 corresponds to a traveling wave also; the dispersion curve associated with this second mode appears as branch 2 in Fig. 3. The shape of this curve is similar to the shapes of the exact flexural dispersion curves of order 2 and higher, in that the phase velocity becomes unbounded as $R/\Lambda \to 0$. For large R/Λ, however, Timoshenko's second branch has the asymptotic value c_0, while all the higher modes in the exact theory have the lower asymptotic value c_S (Rayleigh surface wave velocity) [7]. Further discussion

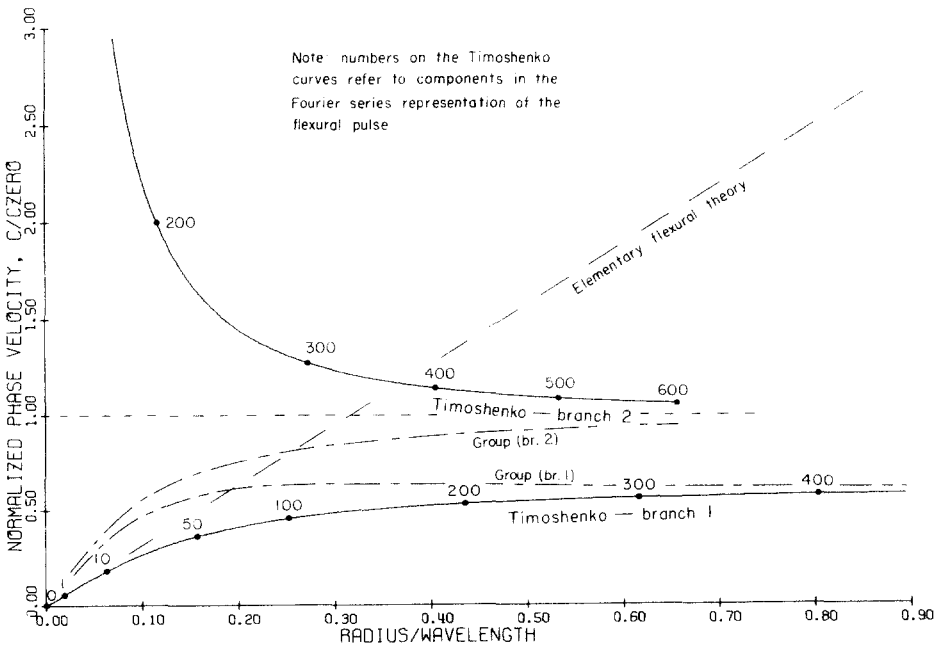

FIG. 3. Phase and group velocity curves for each branch of the Timoshenko theory ($\nu = 0{\cdot}25$).

of Timoshenko's second branch appears later in the paper. For $\omega < \omega_{cr}$, root b_2 corresponds to a spatially decaying wave.

A harmonic solution like (7) may also be assumed for the total angle of rotation $\alpha(x, t)$ of a cross-section, with different constants A_1 and A_2 replacing W_1 and W_2, respectively. From the basic equations of the Timoshenko theory, it can be shown that these four constants are interrelated:

$$-b_1 A_1 = (b_1^2 + \varepsilon' \omega / c_0^2) W_1 \tag{9}$$

$$-b_2 A_2 = (b_2^2 + \varepsilon' \omega^2 / c_0^2) W_2 \tag{10}$$

The two remaining equations needed to determine the four constants uniquely come from the boundary conditions specified at $x = 0$. The moment boundary condition (2) can be satisfied over a finite time interval T_0 by finding unique complex constants M_{on} such that the Fourier series representation

$$M(0, t) = M_{00} + \sum_{n=1}^{\infty} \mathrm{Re}\{M_{on} \exp(i2n\pi t / T_0)\} \tag{11}$$

coincides with the prescribed time dependence. Then since

$$M(x, t) = EI\alpha_{,x}(x, t) \tag{12}$$

there is associated with each (nth) term in (11) an equation of the form

$$-b_1 A_1 - b_2 A_2 = M_0 / EI \tag{13}$$

The vanishing shear resultant condition (4) is met if $w_{,x}(0, t) - \alpha(0, t) = 0$, i.e. if

$$-b_1 W_1 - b_2 W_2 - A_1 - A_2 = 0 \tag{14}$$

The simultaneous solution of equations (9, 10, 13, 14) yields A_1, A_2, W_1 and W_2 in terms of M_0, and appropriate substitution gives the following formula for the moment at any position:

$$M(x, t) = M_{00} + \sum_{n=1}^{\infty} \mathrm{Re}\{[Q_1 \exp(-b_1 x) + Q_2 \exp(-b_2 x)][1/(Q_1 + Q_2)] M_0 \exp(i\omega t) \tag{15}$$

where

$$Q_1 = -b_1[1 - b_2^2/(b_2^2 + \varepsilon' \omega^2 / c_0^2)]$$

and

$$Q_2 = +b_2[1 - b_1^2/(b_1^2 + \varepsilon' \omega^2 / c_0^2)]$$

In equation (15), b_1, b_2 and M_0 are understood to be functions of the summing index n; $\omega = n\omega_0$ where $\omega_0 = 2\pi / T_0$.

NUMERICAL RESULTS

In practice the summation in equation (15) is truncated at some number N determined not only by the desired accuracy in pulse synthesis, but also by the choice of T_0. Flexural waves propagate with a wide range of phase velocities and T_0 must be taken large enough

to insure that negligible interference occurs between the (periodic) pulses Fourier synthesized for $x > 0$. In the present work, T_0 was taken to be

$$T_0 = t_f + 2x_{\max}/c_{\min} \tag{16}$$

where t_f is the original fracture pulse duration $2R/v_c$, $x_{\max}$ is the maximum value of x for which synthesis is desired, and $c_{\min}$ is the phase velocity of first-mode flexural waves for $\omega = \omega_0$. Actually, the first-mode phase velocity approaches zero as $R/\Lambda \to 0$, and for this reason equation (16) should be interpreted as only an estimate for the minimum value of T_0 necessary for reasonably accurate synthesis at $x = x_{\max}$.

Numerical results are presented in Figs. 3 and 4 for a 0·480 in. diameter glass rod with $x_{\max} = 6{\cdot}19$ in. These dimensions coincide with experimental data presented later. For the crack velocity v_c, the theoretical limiting value [8] of $0{\cdot}38\, c_0$ is assumed.

The phase velocity curves in Fig. 3 have been discussed earlier. Also shown in Fig. 3 are the associated group velocity curves [3]

$$c_g = c - \Lambda\, dc/d\Lambda$$

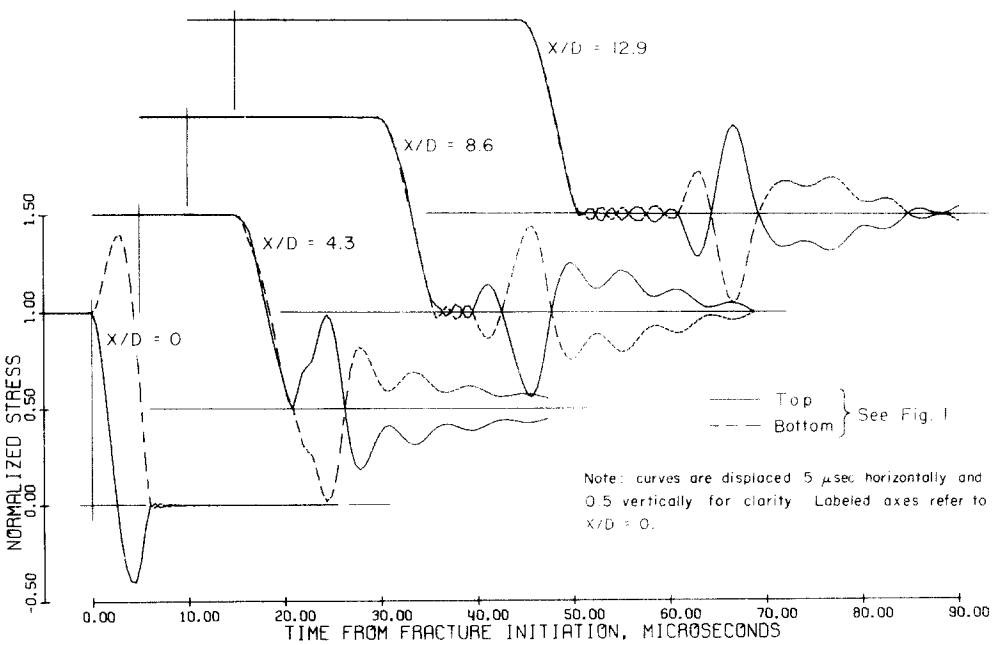

FIG. 4. Time variation of the synthesized axial stresses at $y = \pm R$ for various positions x.

for the two Timoshenko branches. For branch 1, c_g has its maximum value of about $0{\cdot}639\, c_0$ at $R/\Lambda \simeq 0{\cdot}36$. For branch 2, c_g is a monotonically increasing function having the asymptotic value c_0 for large R/Λ.

The synthesized stress vs. time curves at various positions x are shown in Fig. 4. For each value of x, the solid and dashed curves correspond to the extreme fiber stresses

$$\sigma = F(x, t)/A_0 \pm M(x, t)R/I$$

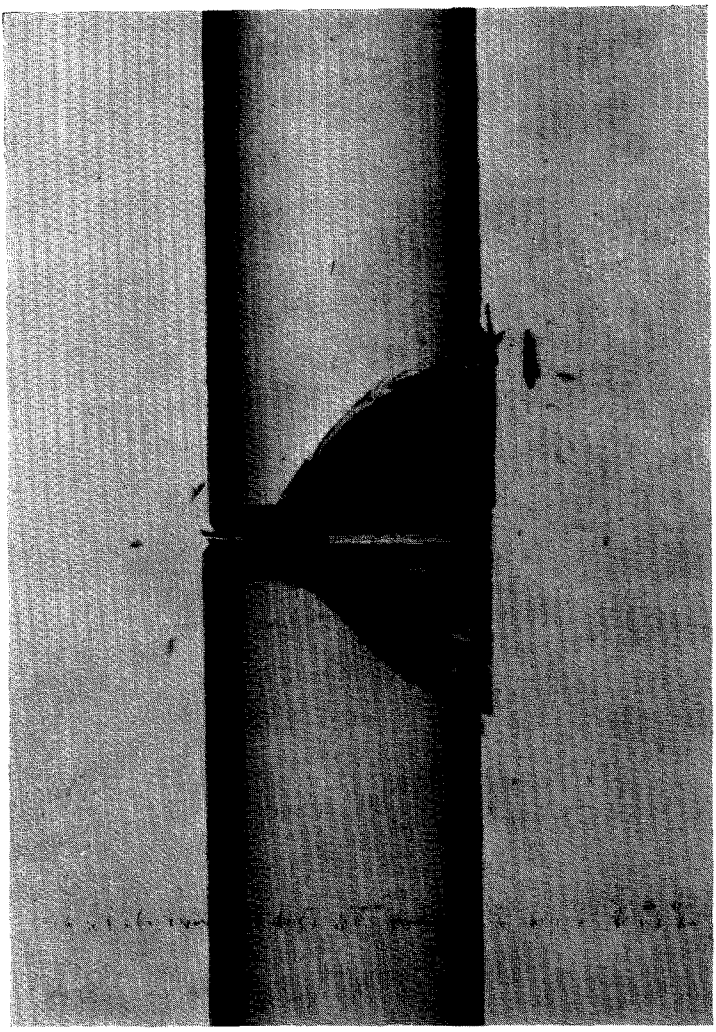

FIG. 5. Typical fracture pattern in a 0·5 in. diameter notched glass rod tensile specimen. Notch is at center left.

facing p. 1408

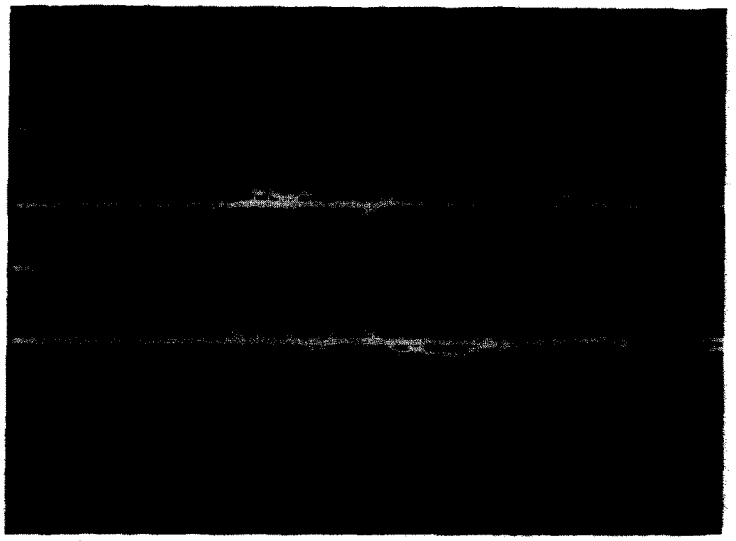

FIG. 6. Individual strain gage responses at $x = 6{\cdot}19$ in. in a 0·480 in. diameter notched glass rod tensile specimen pulled to failure. Upper and lower traces correspond to $y = \mp R$, respectively. Sensitivity = 5 mV/cm, sweep rate = 10 μsec/cm.

for $y = \pm R$, respectively. The longitudinal and flexural pulses are coincident in time at $x = 0$ and tend to separate as they propagate, apparently owing to the fact that the group velocities for both branches of the Timoshenko theory are less than c_0 for all finite R/Λ.

Small oscillations are observed in Fig. 4 at $x/D = 0$ in the approximate time range of 6–10 μsec. These oscillations, whose amplitude is less than 2 per cent of the maximum flexural pulse amplitude, are due to truncation of the Fourier series at a finite N, in this case 600. For these calculations, $T_0 = 991$ μsec and thus the highest frequency component has a period of 1·65 μsec, roughly $\frac{1}{4}$ the width of the flexural pulse. Additional computations have shown that increasing N reduces this oscillation but otherwise leaves the results in Fig. 4 unaltered.

The curves in Fig. 4 labeled $x/D = 12{\cdot}9$ correspond to $x = x_{max}$. Here the longitudinal pulse is clearly distinguished from the trailing flexural pulse. For this x, the minimum expected arrival time of a flexural pulse containing only branch 1 excitation would be 46·3 μsec (based on the maximum group velocity), and indeed the main part of the flexural disturbance arrives at this time. A flexural pulse containing only branch 2 excitation could be expected to arrive with the longitudinal pulse, i.e. at $t = x/c_0$ or 29·6 μsec. The oscillations which appear in the wake of the longitudinal pulse and ahead of the main flexural pulse are attributed to this second branch since the arrival times and wavelengths of small segments of these oscillations correspond well with the branch 2 group velocity curve.

A characteristic feature of all the main flexural pulses synthesized for $x > 0$ is the appearance of a slowly decaying, oscillatory component of nearly constant frequency. A combination of factors is believed to be responsible for this behavior. First, the frequency of these oscillations is extremely close to the critical frequency ω_{cr} at which root b_2 in equation (7) vanishes. Now when b_2 (regardless of its type) is small in comparison with b_1, the coefficient Q_2 in equation (15) is likewise negligible in comparison with Q_1. This implies that, for frequencies in the neighborhood of ω_{cr}, nearly all the energy of the original pulse goes into the first mode; whereas for other frequencies, the energy is shared between the modes. Second, it happens that the duration of the original pulse and the critical period $2\pi/\omega_{cr}$ are of the same order of magnitude, so that Fourier components with frequencies in this critical range are important in characterizing the pulse.

The present results of beam theory are only applicable to sufficiently large values of x/D (say greater than 2). Later comparison with experimental results is made in a region where beam theory is expected to apply.

EXPERIMENT

Tensile tests have been conducted on notched glass rods having a nominal diameter of 0·5 in. The rods varied in length between 8 and 18 in. They were pulled slowly at constant cross-head velocity in an Instron tester, and were observed to fracture at 1050 lb $\pm$ 10 per cent, corresponding to a nominal stress roughly $\frac{1}{3}$ the quoted static ultimate tensile stress [10]. The fracture pattern was found to be extremely reproducible and fairly insensitive to the type of notch employed. The typical fracture shown in Fig. 5 bears a strong resemblance to the fractures in plates under uniaxial loading [11], and is characterized by multiple chips, each chip containing several incomplete fracture surfaces. A delay of 1000 μsec $\pm$ 1 per cent was imposed between the approximate initiation time and the taking of the picture in order to study the rigid-body motion of the chips. The crack-initiating notch is on the left-hand side in this photograph.

For triggering purposes, a thin coat of silver paint was applied around the notch and across the expected crack path. With a battery and resistor, this conducting paint completed what was found to be a dependable triggering circuit, although the signal produced was delayed from the time of fracture *initiation* by about the time required for crack propagation through the paint area (approximately 3 μsec).

For pulse detection in the specimen, diametrically opposed wire strain gages with a gage length of 0·12 in. were mounted at various distances from the notch. They were oriented to measure axial surface strains at the positions $y = \pm R$, and were instrumented so as to permit the placing of approximate zero-strain traces on the Tektronix 551 dual-beam oscilloscope prior to loading. A typical pair of unloading strain traces appears in Fig. 6. Between the third and fourth cm in each trace, the longitudinal (symmetric) pulse arrives and reduces the strain from the pre-fracture level to zero. (The zero-strain traces are only approximately positioned vertically. Glass is a poor conductor of heat and consequently the strain gages operate at elevated temperature; the outputs were observed to vary slowly, apparently in response to air currents near the specimen. Except for a vertical shift of the entire trace, this slow fluctuation is of no importance in the dynamic measurements.) After the longitudinal unloading pulse passes, the strains remain at the zero level until the arrival of an antisymmetric disturbance near the beginning of the fifth cm. In the ninth cm, a partial reflection of the longitudinal pulse from the specimen holder is observed.

COMPARISON AND DISCUSSION

Comparison of the experimental pulses with those predicted theoretically is presented in Fig. 7, where the experimental curve has been shifted both horizontally and vertically (to account for the inherent triggering delay and thermal fluctuations, respectively). The longitudinal pulse, as well as the main part of the flexural pulse, is observed to follow the theoretical prediction remarkably well.

The flexural "precursor" waves corresponding to branch 2 excitation in the Timoshenko theory are not observed experimentally. (The dip in the experimental curve between 40 and 43 μsec in Fig. 7 is a symmetric disturbance.) Also, high frequency oscillations are observed in the wake of the experimental flexural pulse, but their frequency does not correspond to the branch 2 critical frequency mentioned in the theory. These comparisons might suggest

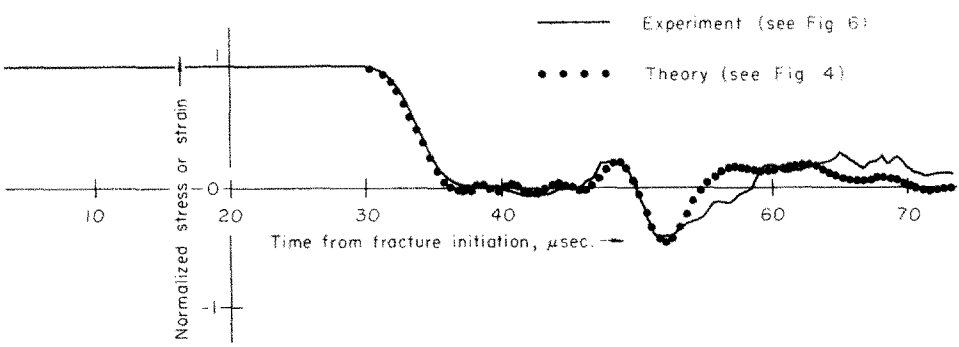

FIG. 7. Comparison of theoretical axial stress and experimental axial strain for $x/D = 12{\cdot}9$, $y = -R$.

that incorporation of the second branch of Timoshenko's theory into the present calculations is unnecessary. However, failure to incorporate the second mode makes it impossible to satisfy the zero shear resultant condition (4), and leads to the prediction of a main (branch 1) flexural pulse whose amplitude is approximately $1\frac{1}{2}$ times larger than the one shown in Fig. 7.

At this point, a careful examination of the assumptions used in the theoretical model is in order. The assumption of a constant crack velocity near the limiting value is felt to be justified because the experimental fracture pattern shows almost immediate bifurcation of the cracks from the notch region [11, 12]. Also justified to some extent is the assumption that axial stresses everywhere in front of the propagating crack remain constant, in view of photoelastic results for plates [13] in which this was found to be approximately true except in the region of the crack tip itself.

Probably the most drastic simplification made in the theoretical analysis is that the fracture is restricted to a single perpendicular plane. The broken specimen reveals a planar crack only in the immediate neighborhood of the notch root. (For smaller specimen diameters or for specimens broken at lower stress levels, the ratio of the planar crack area to the cross-sectional area may be larger.) Bifurcation and the formation of chips soon dominate the fracture pattern, as seen in Fig. 5. Furthermore, the chips are ejected in the negative y-direction with finite velocity, indicating that a non-zero resultant shearing force acts on the remaining specimen, contrary to the vanishing shear condition (4) which follows from symmetry in the theoretical model.

Assumptions other than those used in the present analysis could be used to generate longitudinal and flexural pulses similar to the ones described here. The agreement between theory and experiment (Fig. 7) shows that the assumptions made here give an adequate description of the release pulses which propagate in the rod.

CONCLUSIONS

A glass rod tensile specimen with a suitable surface flaw fractures in a reproducible multi-chip fashion and sustains not only an unloading longitudinal (symmetric) pulse propagating axially away from the fracture zone, but also a flexural (anti-symmetric) pulse whose amplitude in terms of maximum surface strain is of the same order as that of the longitudinal pulse. At a given axial position, the amplitudes, shapes and arrival times of these longitudinal and flexural pulses can be predicted remarkably well by combining approximate pulse propagation theories with a simple fracture model in which cleavage is restricted to a plane normal to the rod axis. Specifically, Timoshenko's beam theory is found to apply. Incorporation of the second mode leads to certain oscillatory features not observed experimentally, and serves principally to reduce the amount of energy propagated in the first mode.

It is concluded that the fracture model proposed is adequate for predicting the longitudinal and flexural pulse propagation in the rod.

Acknowledgements—It is a pleasure to acknowledge many valuable discussions with Professor H. Kolsky, who suggested this problem for analysis. Professor R. J. Clifton read the original work [2] and suggested improvements which were incorporated into this paper. Appreciation is also extended to Messrs. L. Daubney and R. Stanton for their technical assistance. This work was supported by the National Science Foundation under contract GK-749 with Brown University.

REFERENCES

[1] KOSHIRO OI, Transient response of bonded strain gages. *Exp. Mech.* **6**, 463 (1966).
[2] J. W. PHILLIPS, The stress pulses produced by brittle fracture of rods, Brown University report NSF-GK-749/8 (1968). See also J. W. PHILLIPS, Stress waves produced by brittle fracture of rods, Proceedings of the 12th International Congr. of Appl. Mech., Stanford University (August 1968) (Abstract only).
[3] H. KOLSKY, *Stress waves in solids*. Clarendon Press (1953). Also Dover reprint (1964).
[4] D. BANCROFT, The velocity of longitudinal waves in cylindrical bars. *Phys. Rev.* **59**, 588 (1941).
[5] R. M. DAVIES, A critical study of the Hopkinson Pressure Bar. *Phil. Trans. R. Soc.* **240(A)**, 375 (1948).
[6] G. E. HUDSON, Dispersion of elastic waves in solid circular cylinders. *Phys. Rev.* **63**, 46 (1943).
[7] H. N. ABRAMSON, H. J. PLASS and E. A. RIPPERGER, Stress wave propagation in rods and beams. *Adv. Appl. Mech.* **5**, 111 (1958).
[8] D. K. ROBERTS and A. A. WELLS, The velocity of brittle fracture. *Engineering, Lond.* **178**, 820 (1954).
[9] D. RADER, On the dynamics of crack growth in glass. *Exp. Mech.* **6**, 321 (1966).
[10] H. KOLSKY and D. RADER, Stress waves and fracture, Chapter in *Treatise on Fracture*, p. 533, edited by H. LIEBOWITZ. Academic Press (1968).
[11] A. B. J. CLARK and G. R. IRWIN, Crack propagation behaviors. *Exp. Mech.* **6**, 485 (1966).
[12] E. H. YOFFE, The moving Griffith crack. *Phil. Mag.* **42**, 739 (1951).
[13] A. A. WELLS and D. POST, The dynamic stress distribution surrounding a running crack—A photoelastic analysis. *Proc. Soc. Exp. Stress Analysis* **16**, 69 (1958).
[14] Y. M. TSAI and H. KOLSKY, A study of the fractures produced in glass blocks by impact. *J. Mech. Phys. Solids* **15**, 263 (1967). See also Y. M. TSAI, A note on the surface waves produced by Hertzian impact. *J. Mech. Phys. Solids* **16**, 133 (1968).
[15] J. MIKLOWITZ, Elastic waves created during tensile fracture—The phenomenon of a second fracture. *J. appl. Mech.* **20**, 122 (1952).

(*Received* 20 *October* 1969; *revised* 2 *February* 1970)

Абстракт—В целью описания разрушения разтягиваемых образцов предполагаетя теоретическая модель подобная модели использованной Микловцем. В предложенной модели как симметрические так и антисимметрические импульсы распространяются далеко от зоны разрушения. Находится, что теоретические предположенит, касающиеся поверхностных деформаций, замачательно согласны с экспериментальными результатами.